Supporting Information for

Molecular Junctions: Can Pulling Influence Optical Controllability?

Shane M. Parker,[1] Manuel Smeu,[1] Ignacio Franco,[2] Mark A. Ratner,[1] and Tamar Seideman[1, a)]

[1)]*Department of Chemistry, Northwestern University, Evanston, IL 60208, USA*

[2)]*Department of Chemistry, University of Rochester, Rochester, NY 14627, USA*

I. PARAMETER FITTING

In this section we compare several of the computed parameters to the corresponding fits, starting with the fit of the potential energy itself. The 2D potential energy surface was fit to the form

$$\mathcal{V}(l,\beta) = V_0(l) + V_2(l)\cos(2\beta) + V_4(l)\cos(4\beta) + V_6(l)\cos(6\beta) + V_8(l)\cos(8\beta), \tag{1}$$

where V_i are polynomial fits. Several slices of the relaxed potential energy surface are shown in Fig. 3 in the main text. In Fig. S1, we show the computed and fitted values of all the V_i.

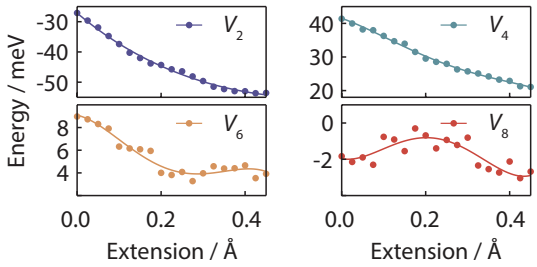

FIG. S1: Comparison of the computed Fourier coefficients at different extensions (circles) and the polynomial fits (lines).

Next, the computed values and the linear fits of the polarizability anisotropy and of the moment of inertia are shown in Fig. S2.

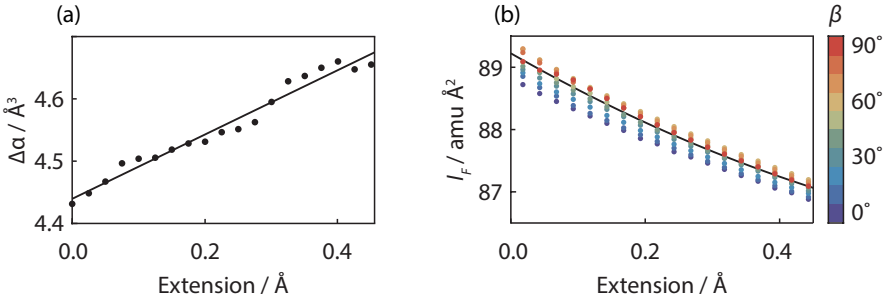

FIG. S2: (a) Comparison of the computed static polarizability anisotropy (circles) and the linear fit (line). The polarizability anisotropy was computed with TD-HF and the def2-TZVP basis set. The dynamic polarizability at a wavelength of 800 nm differed by less than 1%. (b) Comparison of the moments of inertia computed (colored circles) as a function of torsion angle and extension and the polynomial fit (line).

[a)]Electronic mail: t-seideman@northwestern.edu

II. HIGH TEMPERATURE SIMULATIONS

We repeated the same set of simulations and analysis shown in the main text but for an elevated initial temperature of 150K. The results of the quantum dynamics simulations and several of the computed minimum cost paths are shown in Figs. S3 and S4.

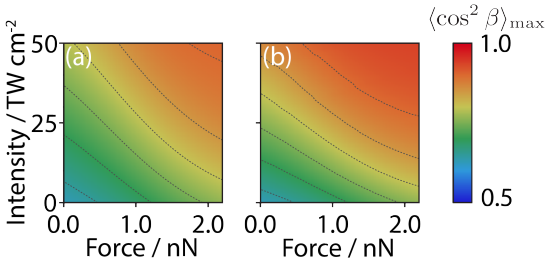

FIG. S3: Maximum achieved $\langle\cos^2\beta\rangle$ as a function of pulling force and field intensity for an ensemble with initial temperature 150 K and a Gaussian pulse, $E(t) = E_0 \exp(-t^2 \ln 2/\tau^2)$, with (a) $\tau = 50$ ps and (b) $\tau = 0.5$ ps.

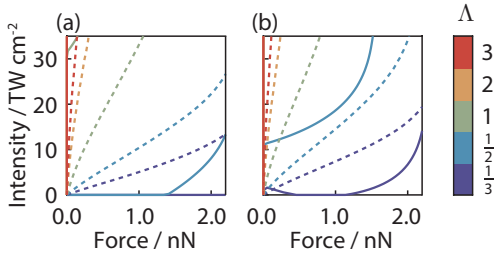

FIG. S4: Linear (solid) and quadratic (dashed) minimum cost paths for Gaussian pulses, $E(t) = E_0 \exp(-t^2 \ln 2/\tau^2)$, with (a) $\tau = 50$ ps and (b) $\tau = 0.5$ ps. The initial temperature in all cases was 150 K. In total, seven values of Λ are plotted from $\Lambda = \frac{1}{3}$ (blue) to $\Lambda = 3$ (red). Those paths not visible lie entirely along either one of the axes (indicating cases in which combining forces is more costly than not).

III. ELECTRON TRANSPORT CALCULATIONS

The geometry of the molecular junction was relaxed as follows. A periodic system was constructed as shown in Fig. S5, which contains the biphenyl dithiol molecule bonded to Au electrode apexes at either end. We used the Vienna *ab initio* simulation package (VASP)[1,2] for the structure relaxations of the electron transport systems. The VASP relaxations used the Perdew-Burke-Ernzerhof generalized gradient approximation (PBE-GGA).[3] The projector augmented wave (PAW) method[4,5] was used to treat the ionic potentials and the plane wave basis was set to a kinetic energy cutoff of 400 eV.

Initially, the two nearest Au layers on either side of the molecule (3 Au atom layer and 6 Au atom layer) were allowed to relax along with all atoms in the molecule, while the 'bulk layer' (identically shown at left and right side of Fig. S5) was held fixed to the bulk Au crystal structure. Structure relaxations were carried out at various electrode-electrode separations to determine the lowest-energy structure. This system corresponds to an electrode-electrode separation of 13.8 Å and is defined as the 0.0 Å extension geometry. The torsional angle in the lowest energy structure is 36° between the two phenyl rings, in excellent agreement with the Q-Chem calculations described in the main text.

From this minimum energy structure, we performed similar relaxations by freezing all Au atoms and stretching the junction by 0.0, 0.1, 0.2 and 0.4 Å. Note that the molecule was allowed to relax at each pulling distance while the Au atoms were not. For each pulling distance, the torsional angle between the two phenyl rings was constrained to 0°, 20°, 36° and 40°. The four torsional angles and four pulling distances gave 16 possible junction geometries to consider in the electron transport calculations. The relaxed junction geometries were used to build two-probe structures, as shown in Fig. S6, by extending the left and right electrodes with Au atoms at the appropriate Au(111) crystal lattice positions. This structure is partitioned into the central region containing the molecule and parts of each electrode, and the left and right electrodes that are semi-infinite and repeat to the left

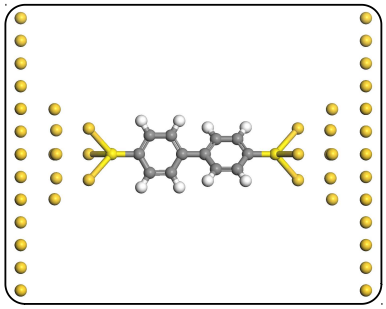

FIG. S5: Periodic structure used for relaxations. Note that leftmost and rightmost Au layers actually correspond to the same atoms due to the periodicity.

and right, respectively. We used the Nanodcal electron transport code[6] which implements the non-equilibrium Green's function formalism within density functional theory (NEGF-DFT).[7,8] This technique has been extensively described in the literature, for examples see Refs. 7–10.

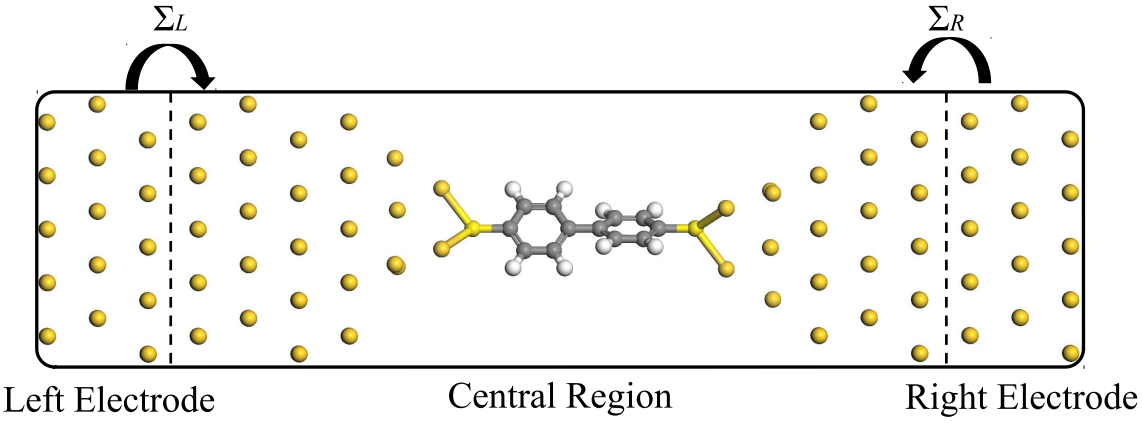

FIG. S6: Two-probe structure used for NEGF-DFT electron transport calculations. The effect of the electrodes on the central region is included in the self energies, $\Sigma_{L/R}$.

The retarded Green's function at energy E is obtained as,

$$G(E) = [ES - H - \Sigma_L - \Sigma_R]^{-1}, \tag{2}$$

where H and S are the Hamiltonian and overlap matrices for the central region, and $\Sigma_{L,R}$ are the self-energies that account for the effect of the left and right electrodes on the central region. These effects are captured by the complex self-energies: the real part represents the shift and the imaginary part represents the broadening in the energy levels of the central region. These are obtained using an iterative technique as described in Ref. 11. The broadening effect of each electrode can be expressed as the line width (or broadening) matrix,

$$\Gamma_{L,R} = i(\Sigma_{L,R} - \Sigma_{L,R}^{\dagger}). \tag{3}$$

With these quantities, we can obtain the electronic density matrix for the central region as,

$$\rho = (1/2\pi) \int_{-\infty}^{\infty} [f(E,\mu_L) G\Gamma_L G^{\dagger} + f(E,\mu_R) G\Gamma_R G^{\dagger}] dE, \tag{4}$$

where $\mu_{L,R}$ are the electrochemical potentials of the left and right electrodes and $f(E,\mu)$ is the Fermi-Dirac function. The density ρ is used in a subsequent DFT step to obtain new H and S quantities, to seed Eq. 2 and the process is repeated until self consistency is achieved. The transmission function can then be obtained from the Green's function as,

$$T(E) = \mathrm{Tr}(\Gamma_L G \Gamma_R G^{\dagger}). \tag{5}$$

This is a probability that an electron with a given energy transmits from one electrode, through the central region, and into the other electrode (see Fig. S6). The value of transmission at the Fermi level of the electrodes, E_{F}, is a good approximation to the low-bias conductance of the molecular junction.

The Nanodcal interpretation of NEGF-DFT uses norm-conserving pseudopotentials[12] to describe the atomic cores; and the valence electrons of Au were treated with a single-ζ polarized basis while a double-ζ polarized basis was used for all other atoms. The basis and density were projected onto a real-space grid with more than five points per Å, k-sampling was carried out on a 3×3 grid in the plane perpendicular to the long axis of the molecule.

Figures S7 and S8 show the transmission spectra (on semi-logarithmic scale) for the 16 junction geometries described in the main text. Figure S7 shows the effect of pulling the molecule at four different torsional angles, while Fig. S8 shows the effect of changing the torsional angle for particular pulling distances. The important result is that the effect on transmission from pulling the molecule is much smaller than the effect of planarizing the molecule. In other words, pulling the molecule to aid in making it planar will have an overall positive effect in increasing conductance.

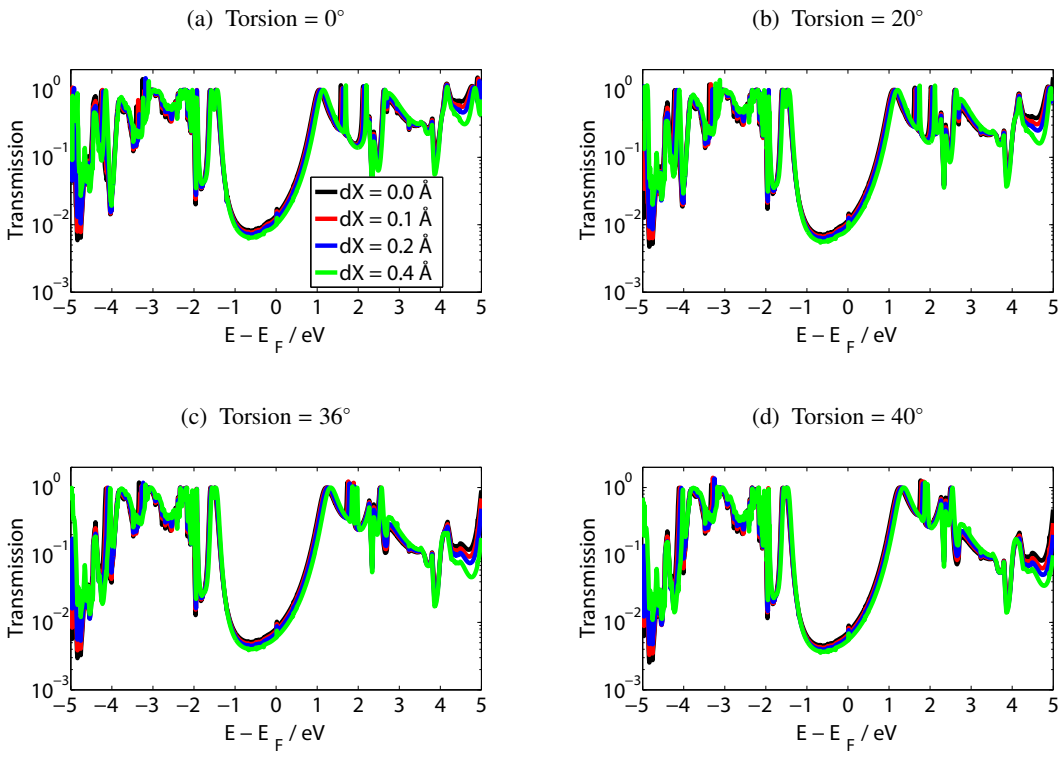

FIG. S7: Transmission for different pulling distances (different colors). Each panel corresponds to a different torsional angle.

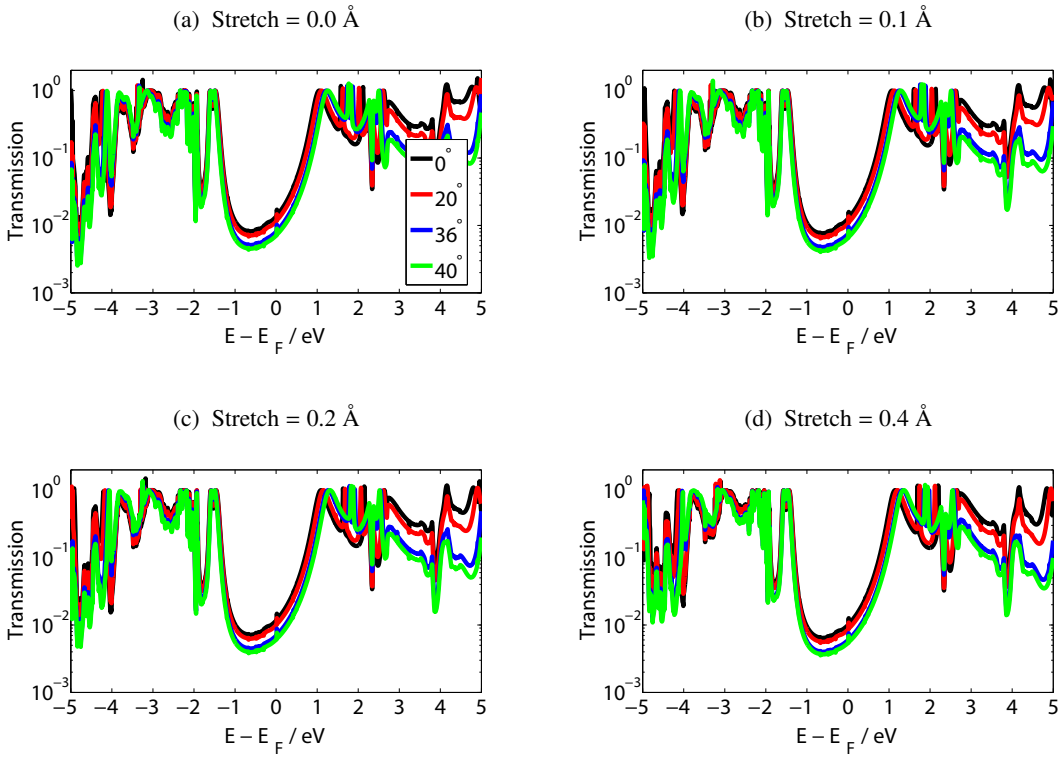

FIG. S8: Transmission for different torsional angles (different colors). Each panel corresponds to a different pulling distance.

REFERENCES

[1] Kresse, G.; Hafner, J. *Phys. Rev. B* **1993**, *47*, 558–561.
[2] Kresse, G.; Furthmüller, J. *Phys. Rev. B* **1996**, *54*, 11169–11186.
[3] Perdew, J. P.; Burke, K.; Ernzerhof, M. *Phys. Rev. Lett.* **1996**, *77*, 3865–3868.
[4] Blöchl, P. E. *Phys. Rev. B* **1994**, *50*, 17953–17979.
[5] Kresse, G.; Joubert, D. *Phys. Rev. B* **1999**, *59*, 1758–1775.
[6] NanoAcademic Technologies. `http://www.nanoacademic.ca`, Accessed: 2014-02-05.
[7] Taylor, J.; Guo, H.; Wang, J. *Phys. Rev. B* **2001**, *63*, 245407.
[8] Waldron, D.; Haney, P.; Larade, B.; MacDonald, A.; Guo, H. *Phys. Rev. Lett.* **2006**, *96*, 166804.
[9] Saraiva-Souza, A.; Smeu, M.; Terrones, H.; Souza Filho, A. G.; Ratner, M. A. *J. Phys. Chem. C* **2013**, *117*, 21178–21185.
[10] Li, Z.; Smeu, M.; Ratner, M. A.; Borguet, E. *J. Phys. Chem. C* **2013**, *117*, 14890–14898.
[11] Sancho, M. P. L.; Sancho, J. M. L.; Rubio, J. *J. Phys. F: Met. Phys.* **1984**, *14*, 1205.
[12] Troullier, N.; Martins, J. L. *Phys. Rev. B* **1991**, *43*, 1993–2006.